Effect of noise on the dynamics at the torus-doubling terminal point in a quadratic map under quasiperiodic driving

Sergey P. Kuznetsov
Max-Planck-Institut fur Physik Komplexer Systeme, Nothnitzer Straße 38, 01187 Dresden, Germany
and Institute of Radio-Engineering and Electronics of RAS, Saratov Division, Zelenaya 38, Saratov, 410019, Russian Federation
(Received 25 February 2005; published 10 August 2005)

Scaling regularities are examined associated with the effect of additive noise on a system driven by an external quasiperiodic force with the golden-mean frequency ratio near the terminal point of the torus-doubling bifurcation curve (TDT point). This point was studied in the context of the problem of the onset of a strange nonchaotic attractor on the basis of renormalization group (RG) analysis [Kuznetsov *et al.*, Phys. Rev. E **57**, 1585 (1998)] and observed in experiments with a quasiperiodically driven resistor-inductor-diode circuit [Bezruchko *et al.*, Phys. Rev. E **62**, 7828 (2000)]. The method implemented in the present paper is based on a generalization of the RG approach of Crutchfield *et al.* [Phys. Rev. Lett. **46**, 933 (1981)] and Shraiman *et al.* [Phys. Rev. Lett., **46**, 935 (1981)], originally developed for the period-doubling transition to chaos in the presence of noise. At the TDT point, a constant determining the rescaling rule for the intensity of noise is found to be $\gamma=20.048\,637\,7$. It means that a decrease of the noise amplitude by this factor ensures the possibility of observing one more level of the fractal-like structure of the dynamics, with increase of the characteristic time scale by $[(\sqrt{5}+1)/2]^3$. Numeric results demonstrating evidence of the expected scaling are presented, e.g., portraits of the noisy attractors and Lyapunov charts on the parameter plane in different scales.

DOI: 10.1103/PhysRevE.72.026205 PACS number(s): 05.45.−a, 05.10.Cc, 05.40.Ca

I. INTRODUCTION

In nonlinear dynamics the renormalization group (RG) approach was introduced by Feigenbaum [1] and later applied successively for analysis of different types of transitions to chaos, e.g., via period doubling [1,2], intermittency [3], and quasiperiodicity [4]. As commonly recognized, this is an effective and powerful theoretical instrument uncovering deep and fundamental features of the dynamics between order and chaos, like quantitative universality and scale invariance (scaling) for subtle fractal structures in phase space and in parameter space, which are associated with the transitions.

In the class of quasiperiodically forced dissipative systems a typical attribute of the dynamics between order and chaos is the occurrence of a strange nonchaotic attractor (SNA). Therefore, it is natural to expect that RG analysis may be relevant for understanding the nature of SNAs, the mechanisms of their creation, and, perhaps, for fundamental quantitative regularities intrinsic to these phenomena. Originally, this idea was advanced in [5], and later it was applied to several types of critical points in parameter space of quasiperiodically driven maps with the golden-mean frequency ratio [critical points of the torus-doubling terminal (TDT) [6], torus-collision terminal [7], and torus fractalization (TF) [8]]. Dynamics near the TDT critical point was actualized and observed in experiment with quasiperiodically driven resistor-inductor (RL) diode circuit [9]. The Occurrence of the TF critical point in a model of a driven Josephson junction was validated numerically in Ref. [10].

In real physical systems one must account for the inevitable noise, which obliterates fine details of fractal-like self-similar structures in phase space and parameter space associated with transitions to chaos or SNA. Thus, understanding the effect of noise is a problem of crucial significance, e.g., for analysis and interpretation of experimental studies of these transitions.

A theoretical approach to the description of the effect of noise based on a RG analysis was suggested first by Crutchfield *et al.* and Shraiman *et al.* [11] in application to the period-doubling transition to chaos in dissipative systems. They obtained a universal factor $\gamma=6.619\,036\ldots$ responsible for the scaling properties of the transition with respect to the effect of noise; namely, a decrease of the amplitude of noise by that factor ensures the possibility of observing one more level of the period doubling. Later, analogous approaches were developed and corresponding scaling factors estimated for many other types of critical behavior, e.g., for period doubling in conservative systems and area-preserving maps [12], for bicritical behavior of unidirectionally coupled period-doubling systems [13], for transition to chaos via the golden-mean quasiperiodicity in dissipative [14] and conservative [15] systems, and for the period-tripling cascade in complex analytic maps [16].

This paper is devoted to the problem of the effect of noise on dynamics at the TDT critical point introduced and studied in the work of Kuznetsov, Feudel, and Pikovsky [6]. The basic model is a quasiperiodically driven quadratic map [18]

$$x_{n+1} = \lambda - x_n^2 + \varepsilon \cos 2\pi u_n,$$

$$u_{n+1} = u_n + w \pmod 1, \tag{1}$$

where $w=(\sqrt{5}-1)/2$ is the inverse golden-mean constant. The TDT point is located at

$$\lambda_c = 1.158\,096\,856\,726, \quad \varepsilon_c = 0.360\,248\,020\,507. \quad (2)$$

One more relevant value for the model (1) is a "scaling center" for the phase variable,

$$u_c = 0.395\,218\,826\,46. \quad (3)$$

At this phase the critical attractor at the TDT point touches the extremum of the map $x=0$ and is characterized by a property of self-similarity in respect to scale change along the axes x and u with the following factors extracted from the RG analysis:

$$a = 3.963\,766\,561\,57, \quad b = -1/w^3 = -4.236\,067\,977\,50. \quad (4)$$

(I present here improved values in comparison with those in the original work [6].)

Section II is devoted to discussion of some empirical numerical results for the stochastic version of the model (1) with additive noise. In Sec. III RG analysis of the effects of noise on the TDT cicritical behavior is developed. I derive the RG equation and obtain a high-precision value for the universal constant responsible for scaling properties with respect to the noise amplitude. In Sec. IV conclusions following from the RG analysis are discussed in application to the stochastic version of the model system (1). Computer illustrations for scaling regularities are presented including portraits of the noisy attractors and gray-scale charts for the Lyapunov exponent on the parameter plane near the TDT point in different scales and at different noise levels.

II. EFFECT OF NOISE: EMPIRICAL RESULTS

Let us introduce a sequence ξ_n that represents a discrete-time white noise. It means that terms of the sequence at different steps of time are assumed to be statistically independent. The average for ξ_n is zero, $\langle \xi_n \rangle = 0$, and the standard deviation is some constant, $\sigma = \sqrt{\langle \xi_n^2 \rangle}$. Then let us consider the following stochastic map:

$$x_{n+1} = \lambda - x_n^2 + \varepsilon \cos 2\pi u_n + \kappa \xi_n,$$

$$u_{n+1} = u_n + w \pmod 1, \quad (5)$$

where κ characterizes the intensity of the additive noise source.

If the amplitude of noise is small, and behavior on large time scales is examined, the concrete form of the probability distribution for ξ_n appears not to be essential, and the behavior of the noisy system will be of a universal nature (the same is true for other critical situations allowing analysis in terms of the RG method; cf. [17]). In derivation of the RG equations in the next section I will assume the noise to be Gaussian. In computations, accounting for the expected universality, I define ξ_n as random numbers uniformly distributed over an interval $[-0.5, 0.5]$. Hence, $\sigma = 1/\sqrt{12}$.

In Fig. 1 Lyapunov charts are shown on the plane of the control parameter λ versus the amplitude of driving ε without noise ($\kappa=0$) and in the presence of noise ($\kappa=0.03$). The Lyapunov exponent has been computed via the relation

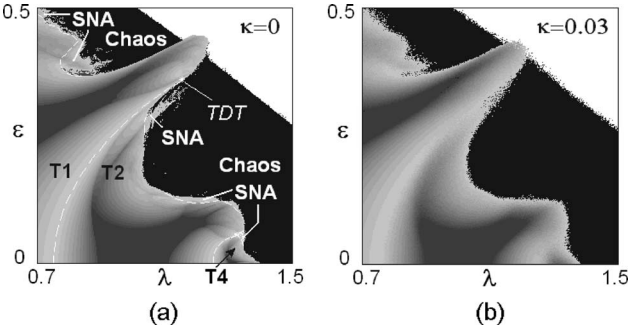

FIG. 1. Lyapunov charts on the plane of control parameter λ versus amplitude of driving ε for the model (5) without noise (a) and in the presence of noise (b). Gray tones designate negative values of the Lyapunov exponent (the lighter the color, the less negative is the exponent). Positive values (chaos) are designated by black. On the panel (a) the nature of the main dynamical regimes is explained with inscriptions in the respective areas (torus $T1$, doubled torus $T2$, SNA, chaos), and the location of the TDT critical point is indicated. The white area in the right top corner corresponds to divergency of the iterations

$$\Lambda \cong N^{-1} \sum \ln|2x_n| \quad (6)$$

at each pixel of the picture. Negative values of Λ are coded in gray scale, The lighter the color, the less negative is the Lyapunov exponent; positive Λ associated with chaotic dynamics are designated by black. Location of the TDT critical point is indicated on the panel (a). Comparing the diagrams (a) and (b) one can observe a result of the effect of noise, which is rather obvious: it obliterates subtle details of the picture of the dynamical regimes. In Fig. 2 portraits of the attractor at the TDT critical point are plotted on iteration diagrams, in coordinates (x_n, x_{n+1}). Diagram (a) corresponds to a pure dynamical case (no noise), diagrams (b) and (c) to the presence of noise of smaller and larger amplitudes, respectively. Diagram (d) is reproduced from Ref. [9] and relates to the experiment with the quasiperiodically driven RL diode circuit. [It is remarkable that the experimental portrait resembles more the noisy attractors (b) and (c) than that without noise.]

III. RENORMALIZATION GROUP ANALYSIS

In application to all situations of the golden-mean quasiperiodisity, the main idea of the RG analysis consists in examination of evolution operators defined for time intervals given by subsequent Fibonacci numbers $F_k: F_0=0, F_1=1, F_{k+2}=F_{k+1}+F_k$.

Let us suppose that in the presence of noise the equations governed dynamics at the TDT point for F_k and F_{k+1} steps of discrete time are

$$x_{i+F_k} = \phi_k(x_i, y_i) + \kappa \xi_i \psi_k(x_i, y_i),$$

$$y_{i+F_k} = y_i + wF_k = y_i - (-w)^k \pmod 1 \quad (7)$$

and

$$x_{i+F_k} = \phi_{k+1}(x_i, y_i) + \kappa \xi_i \psi_{k+1}(x_i, y_i),$$

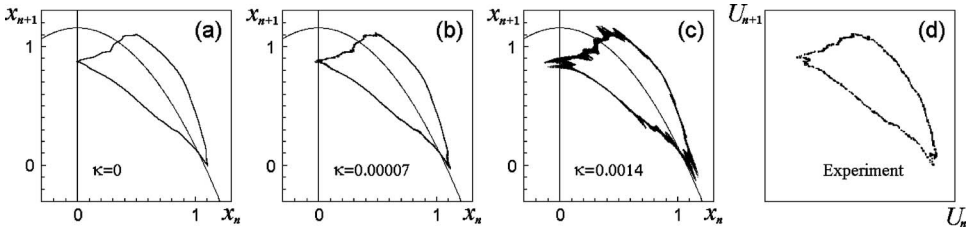

FIG. 2. Portraits of attractor at the TDT critical point (2) on iteration diagrams in coordinates (x_n, x_{n+1}) obtained from computer simulation: diagram (a) corresponds to the pure dynamical case (no noise), diagrams (b) and (c) to the presence of noise of smaller and larger amplitudes, respectively. Diagram (d) is reproduced from Ref. [9] and relates to the experiment with a quasiperiodically driven resistor-inductor-diode circuit.

$$y_{i+F_{k+1}} = y_i + wF_{k+1} = y_i - (-w)^{k+1} \pmod 1, \tag{8}$$

where $y=u-u_c$ is the phase variable measured from a scaling center (3), ξ_i is a random sequence with properties formulated in the previous section, the noise amplitude parameter κ is supposed to be small, and $\psi_k(x,y)$ and $\psi_{k+1}(x,y)$ are some auxiliary functions. Obviously, the model (5) corresponds to a particular version of these relations: at $F_1=F_2=1$ we set

$$\phi_1(x,y) = \phi_2(x,y) = \lambda_c - x^2 + \varepsilon_c \cos 2\pi(y+u_c),$$

$$\psi_1(x,y) = \psi_2(x,y) \equiv 1. \tag{9}$$

By a composition of Eqs. (7) and (8), retaining terms up to the first order in κ, we obtain an equation for evolution over F_{k+2} steps of discrete time:

$$\begin{aligned} x_{i+F_{k+2}} = {} & \phi_k(\phi_{k+1}(x_i,y_i), y_i - (-w)^{k+1}) + \kappa[\xi_i \phi_k'(\phi_{k+1}(x_i,y_i), y_i \\ & - (-w)^{k+1}) \psi_{k+1}(x_i,y_i) + \xi_{i+F_{k+1}} \psi_k(\phi_{k+1}(x_i,y_i), y_i \\ & - (-w)^{k+1})]. \end{aligned} \tag{10}$$

In respect to the stochastic terms, we make the following remark. Let us suppose that at some moment an orbit starts at (x_i,y_i). Consider an ensemble of the Gaussian random numbers $\{\xi_i, \xi_{i+Fk+1}\}$ of zero mean and mean square σ^2, and compose them with coefficients given by functions of (x_i,y_i). As $\{\xi_i, \xi_{i+Fk+1}\}$ are statistically independent, the sum can be represented again as a Gaussian random number of zero mean and mean square σ^2, multiplied by some function of x_i and y_i namely,

$$\begin{aligned} & \xi_i \phi_k'(\phi_{k+1}(x_i,y_i), y_{i+1}) \psi_{k+1}(x_i,y_i) + \xi_{i+F_{k+1}} \psi_k(\phi_{k+1}(x_i,y_i), y_{i+1}) \\ & = \tilde{\xi}_i \psi_{k+2}(x_i,y_i). \end{aligned} \tag{11}$$

Now, we set

$$\phi_{k+2}(x,y) = \phi_k(\phi_{k+1}(x,y), y - (-w)^{k+1}) \tag{12}$$

and rewrite Eq. (10) in a form analogous to Eqs. (7) and (8), with redefined random variable and functions ϕ and ψ:

$$x_{i+F_{k+2}} = \phi_{k+2}(x_i,y_i) + \kappa \tilde{\xi}_i \psi_{k+2}(x_i,y_i). \tag{13}$$

To obtain closed functional equations, we square both parts of Eq. (11) and perform averaging over an ensemble of realizations of the noise. As $\langle \tilde{\xi}_i^2 \rangle = \langle \xi_i^2 \rangle = \sigma^2$ and $\langle \xi_i \xi_{i+F_{k+1}} \rangle = 0$, we come to the relation

$$\begin{aligned} [\psi_{k+2}(x,y)]^2 = {} & [\phi_k'(\phi_{k+1}(x,y), y - (-w)^{k+1})]^2 [\psi_{k+1}(x,y)]^2 \\ & + [\psi_k(\phi_{k+1}(x,y), y - (-w)^{k+1})]^2. \end{aligned} \tag{14}$$

In accordance with the basic content of the renormalization approach, now we implement a scale change $x \mapsto x/\alpha^k$, $u \mapsto (-w)^k u$, where

$$\alpha = \sqrt[3]{a} = 1.582\,593\,423\,013\ldots$$

is the scaling constant for the critical TDT dynamics [6]. Then, in terms of the rescaled functions

$$\begin{aligned} g_k(x,y) &= \alpha^k \phi_k(\alpha^{-k}x, (-w)^k y), \\ f_k(x,y) &= \alpha^k \phi_{k+1}(\alpha^{-k}x, (-w)^k y), \\ \Phi_k(x,y) &= [\psi_k(\alpha^{-k}x, (-w)^k y)]^2, \\ \Psi_k(x,y) &= [\psi_{k+1}(\alpha^{-k}x, (-w)^k y)]^2, \end{aligned} \tag{15}$$

the above equations imply that

$$\begin{aligned} g_{k+1}(x,y) &= \alpha f_k(x/\alpha, -wu), \\ f_{k+1}(x,y) &= \alpha g_k(f_k(x/\alpha, -wu), -wu + w), \\ \Phi_{k+1}(x,y) &= \alpha^2 \Psi_k(x/\alpha, -wu), \\ \Psi_{k+1}(x,y) &= \alpha^2 \{[g_k'(f_k(x/\alpha, -wu), -wu + w)]^2 \Psi_k(x/\alpha, -wu) \\ & \quad + \Phi_k(f_k(x/\alpha, -wu), -wu + w)\}. \end{aligned} \tag{16}$$

These relations define the RG transformation for a set of functions $\{g_k, f_k, \Phi_k, \Psi_k\}$. The procedure may be repeated again and again to get the functions for larger and larger k, i.e., to determine the renormalized evolution operators for the set $\{g_k, f_k, \Phi_k, \Psi_k\}$ at larger Fibonacci numbers of steps of discrete time F_k.

As follows from the RG analysis undertaken in Ref. [6], at the TDT critical point, the sequence of functions $g_k(x,y)$, $f_k(x,y)$ converges asymptotically to a period-3 fixed-point solution of the RG equation $\{(g_1,f_1),(g_2,f_2),(g_3,f_3)\}$, which obeys

$$g_2(x,y) = \alpha f_1(x/\alpha, -wy),$$

$$f_2(x,y) = \alpha g_1(f_1(x/\alpha, -wy), -wy + y),$$

$$g_3(x,y) = \alpha f_2(x/\alpha, -wy),$$

$$f_3(x,y) = \alpha g_2(f_2(x/\alpha, -wy), -wy + y),$$

$$g_1(x,y) = \alpha f_3(x/\alpha, -wy),$$

$$f_1(x,y) = \alpha g_3(f_3(x/\alpha, -wy), -wy + y), \tag{17}$$

or

$$g_3(x,y) = \alpha^2 g_1(\alpha^{-1} g_2(x/\alpha, -wy), w^2 y + w),$$

$$g_1(x,y) = \alpha^2 g_2(\alpha^{-1} g_3(x/\alpha, -wy), w^2 y + w),$$

$$g_2(x,y) = \alpha^2 g_3(\alpha^{-1} g_1(x/\alpha, -wy), w^2 y + w). \tag{18}$$

Numerical data for polynomial expansion of the universal functions $g_{1,2}(x,y)$ (over even powers of x and all integer powers of y) may be found in Ref. [19].

Convergence of the functions g and f to the period-3 solution of the RG transformation implies that the recursive linear functional equations for the functional pairs $\{\Phi_k(x,y), \Psi_k(x,y)\}$ is determined asymptotically by an eigenvector associated with the largest eigenvalue Ω for the eigenproblem

$$\Omega \begin{pmatrix} \Phi \\ \Psi \end{pmatrix} = \hat{R}_3 \hat{R}_2 \hat{R}_1 \begin{pmatrix} \Phi \\ \Psi \end{pmatrix}, \tag{19}$$

where $\hat{R}_k$ are linear operators expressed, in accordance with the right-hand parts of the two last equations (16), as

$$\hat{R}_k \begin{pmatrix} \Phi \\ \Psi \end{pmatrix} = \begin{pmatrix} \alpha^2 \Psi(x/\alpha, -wu) \\ \alpha^2 \{[g_k'(f_k(x/\alpha, -wu), -wu + w)]^2 \Psi(x/\alpha, -wu) + \Phi(f_k(x/\alpha, -wu), -wu + w)\} \end{pmatrix}. \tag{20}$$

As mentioned, the universal functions $g_k(x,y)$ are known from numerical solution of the set of functional equations (18) in the form of expansion over powers of the arguments [6,19]. Using these data, I have constructed the functional transformation of the right-hand part of Eq. (19) as a computer program. The unknown functions $\{\Phi(x,y), \Psi(x,y)\}$ were represented by a set of their values at nodes of a grid in a rectangular $\{-1.2 < x < 1.2, -w < y < 1\}$, and by an interpolation scheme between them. Taking random initial conditions for $\{\Phi(x,y), \Psi(x,y)\}$, the program performed the functional transformation many times and normalized the resulting functions at each step as $\Phi^0(x,y) = \Phi(x,y)/\Phi(0,0), \Psi^0(x,y) = \Psi(x,y)/\Phi(0,0)$, until the form of the functions stabilized. The value of $\Phi(0,0)$ (before the normalization) converges to the eigenvalue

$$\Omega = 401.947\,874\,114. \tag{21}$$

Now, in linear approximation with respect to the noise amplitude, the stochastic map for the evolution over F_{3k+q} and F_{3k+q+1} steps at the TDT critical point may be written in terms of the renormalized variables at large k as

$$x_{i+F_{3k+q}} = g_q(x_i, y_i) + \kappa \gamma^k \xi_i \varphi_q(x_i, y_i), \quad y_{i+F_{3k+q}} = y_i - 1, \tag{22}$$

where $q = 1, 2, 3$ and

$$\varphi_q(x,y) = \sqrt{\Phi_q^0(x,y)}, \quad \gamma = \sqrt{\Omega} = 20.048\,637\,712. \tag{23}$$

Next, if we consider a small shift of parameters λ and ε from the TDT critical point, some additional perturbation terms will appear in the equations, which correspond to two relevant eigenmodes of the RG equation linearized at the period-3 fixed point solution (see [6]). With account of them and of noise we have to write

$$x_{i+F_{3k+q}} = g_q(x_i, y_i) + C_1 \delta_1^k h_q^{(1)}(x_i, y_i) + C_2 \delta_2^k h_q^{(2)}(x_i, y_i) + \kappa \gamma^k \xi_i \varphi_q(x_i, y_i), \tag{24}$$

where $q = 1, 2, 3$ and $\{h_1^{(1)}(x,y), h_2^{(2)}(x,y), h_3^{(1)}(x,y)\}$ and $\{h_1^{(2)}(x,y), h_2^{(2)}(x,y), h_3^{(2)}(x,y)\}$ are the respective egenfunvectors. The eigenvalues δ_1 and δ_2 have been presented in Ref. [6]; here I give the improved numerical results:

$$\delta_1 = 10.502\,983\,5, \quad \delta_2 = 5.188\,118\,1. \tag{25}$$

The coefficients C_1 and C_2 in Eq. (24) depend on the parameters of the original map and vanish at the TDT critical point. In a close neighborhood of the critical point it is sufficient to account for only the leading, linear terms of the expansions in respect to the original parameters, proportional to $\lambda - \lambda_c$ and $\varepsilon - \varepsilon_c$.

Now, we are ready to formulate the basic scaling property of the dynamics near the TDT point in the presence of noise that follows from Eq. (24).

If we decrease the parameter shift from the TDT point in such a way that the coefficients C_1 and C_2 are reduced by factors δ_1 and δ_2, respectively, and decrease the noise amplitude κ by a factor γ; then the form of the stochastic map (24) remains unchanged. Thus, at the new parameters, the noisy system will demonstrate statistically similar behavior as at the old ones, but with a characteristic time scale multiplied by $F_{k+3}/F_k \cong W^3 = [(\sqrt{5}+1)/2]^3$.

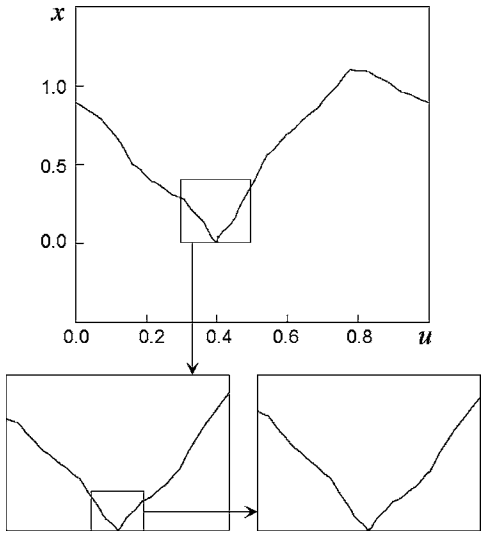

FIG. 3. Attractor of the forced quadratic map (1) at the TDT critical point (the top panel) and illustration of the basic local scaling property: the structure reproduces itself under magnification with factors $a=3.963\,76\ldots$ and $b=W^3=4.2360\ldots$ along the vertical and the horizontal axes, respectively.

IV. SCALING PROPERTIES AND THEIR DEMONSTRATION IN NUMERICAL COMPUTATIONS

Now let us discuss some manifestations of the effects of noise on dynamics of the model map (5) at the TDT point and in its vicinity in numerical experiments in view of the scaling properties stated in the previous section.

A. Noisy critical attractor

In the presence of noise, the subtle structure of the attractor is smeared out level by level, as the intensity of noise grows. In accordance with the conclusions of the previous section, each new level of the structure blurs when we increase the magnitude of the noise source by factor γ.

To examine scaling properties of the critical attractor at the TDT point it is convenient to use a graphical representation on the phase plane (u,x) rather than on the iteration diagram as done in Sec. II. Without noise, the attractor looks like a kind of fractal curve (Fig. 3). To reveal its true fractal nature, let us note, first, that it manifests a nontrivial property of self-similarity near the scaling center $x=0, u=u_c$. Indeed, if one rescales x and $y=u-u_c$, respectively, by factors $a=3.9367\ldots$ and $b=w^{-3}=4.2360\ldots$, the curve must be locally invariant under this transformation as follows from the RG analysis of Ref. [6]. As seen from Fig. 3, this is indeed the case: the picture inside a selected box reproduces itself under subsequent magnifications by these factors. To possess the scaling property, the curve must behave locally as $x\propto|\Delta u|^{\rho}$ with $\rho=\ln a/\ln b\cong 0.954$. The exponent ρ is close to 1, so visually the curve looks broken at the point of singularity. Due to ergodicity of the quasiperiodic motion, the singularity of the invariant curve at the origin implies the presence of singularities of the same type at all preimages of this point. Due to the quasiperiodic nature of the motion, they occupy a dense set of points on the invariant curve. As ρ is less than 1, it follows that the invariant curve is nowhere differentiable, i.e., it is fractal.

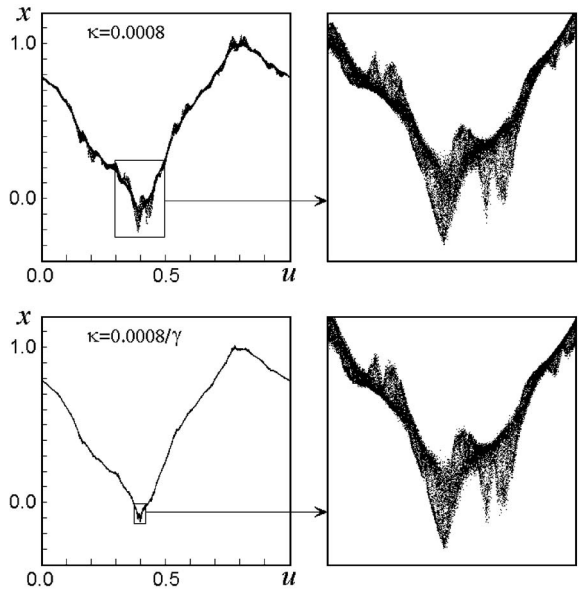

FIG. 4. Portraits of the noisy attractors of the model system (5) at the TDT critical point $\lambda=\lambda_c=1.158\,096\,8\ldots$, $\varepsilon=\varepsilon_c=0.360\,248\,4\ldots$ at a larger (a) and smaller (b) noise intensity parameter κ. The right-hand panels represent boxes from the previous diagrams, with a magnification that differs for the plots (a) and (b) by factors $a=3.963\,76\ldots$ and $b=-W^3=-4.2360\ldots$ along the vertical and horizontal axes, respectively

Figure 4 shows portraits of the noisy attractors of the model system (5) at the TDT critical point at the noise intensity parameter $\kappa=0.0008$ (a) and $\kappa=0.0008/\gamma\approx 0.000\,04$ (b). Right-hand panels represent small boxes from the previous diagrams with enlargement. In comparison with diagram (a) the magnification for the plot (b) is increased by factors a and b along the vertical and horizontal axes, respectively. Observe the similarity of the pictures in the right-hand panels.

B. Lyapunov exponent in the presence of noise

In accordance with the results of Sec. III, at the TDT critical point the system will demonstrate similar behaviors for the noise intensity values κ and κ/γ, but with character-

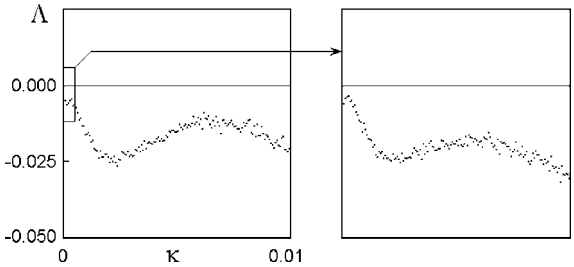

FIG. 5. Plots for the Lyapunov exponent versus the noise intensity κ. A selected box is shown with magnification by the factor $W^3=4.236\ldots$ along the vertical axis, and by the factor $\gamma=20.0486\ldots$ along the horizontal axis.

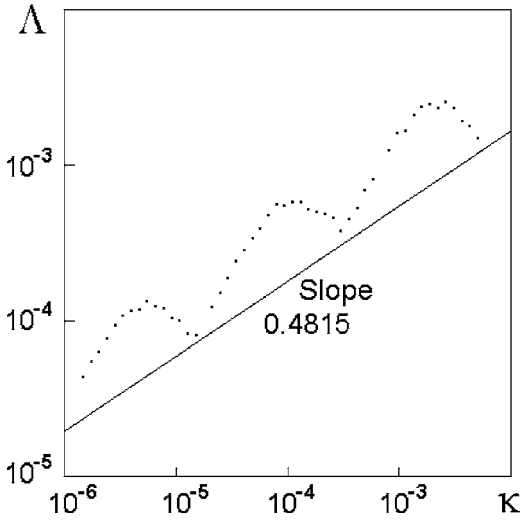

FIG. 6. Plot of the Lyapunov exponent versus noise intensity at the TDT critical point on double logarithmic scale (dots). The straight line slope corresponds to the relation (26).

istic time scale multiplied by $W^3=w^{-3}=4.2360\ldots$ in the second case. Hence, the magnitude of the Lyapunov exponent at κ/γ must be less by this factor than that at κ. Figure 5 shows the plots for the Lyapunov exponent versus the noise intensity κ. A selected box is shown with magnification by a factor W^3 along the vertical axis, and by a factor γ along the horizontal axis. Observe the self-similarity of the pictures under this scale change. Clearly, at smaller scales the degree of coincidence will become better.

Let us estimate a critical index for the Lyapunov exponent with respect to the intensity of noise. Taking account of the fact that a change of κ by a factor γ is accompanied by a change of Lyapunov exponent by a factor W^3, we conclude that the relation must hold,

$$\Lambda \propto \kappa^{\eta} \tag{26}$$

where $\eta=3\log_{\gamma}W=0.481\,506\,953$. Figure 6 shows the dependence of Λ on κ in a double logarithmic scale. The points obtained in numerical computations evidently follow on average a straight line with slope η. The dependence has oscillations, which are of period ln γ along the κ axis in accordance with the scaling law derived from the RG analysis.

It is worth emphasizing a kind of noisy stabilization of the dynamics at the TDT point. Indeed, the effect of noise at the TDT point promotes a decrease of the Lyapunov exponent, i.e., a decrease of sensitivity with respect to the initial conditions, and delays the onset of chaos.

C. Self-similar arrangement of a vicinity of the TDT point in the parameter plane for the noisy system

As mentioned, the structures visible on the Lyapunov chart blur out as the intensity of noise grows (see Fig. 1). On the basis of the scaling arguments of Sec.III we can reveal now a quantitative aspect of this effect.

To observe the scaling regularities in the vicinity of the critical point we need to define an appropriate local coordinate system ("scaling coordinates"). As origin, we naturally take the TDT point itself. Then, the coordinate axes should be directed in such a way that a shift along the first axis gives rise to the mode of perturbation of the evolution operators associated with eigenvalue δ_1 of the linearized RG transformation, and a shift along the second axis produces the mode with δ_2. In fact, an axis corresponding to the larger eigenvalue δ_1 may be defined almost arbitrarily, say, along the λ axis in the original coordinates, but the second one must be selected carefully to exclude a contribution of the first eigenmode in the solution. As found numerically, for the model (5), appropriate new coordinates (c_1,c_2) and parameters (λ,ε) are linked as follows:

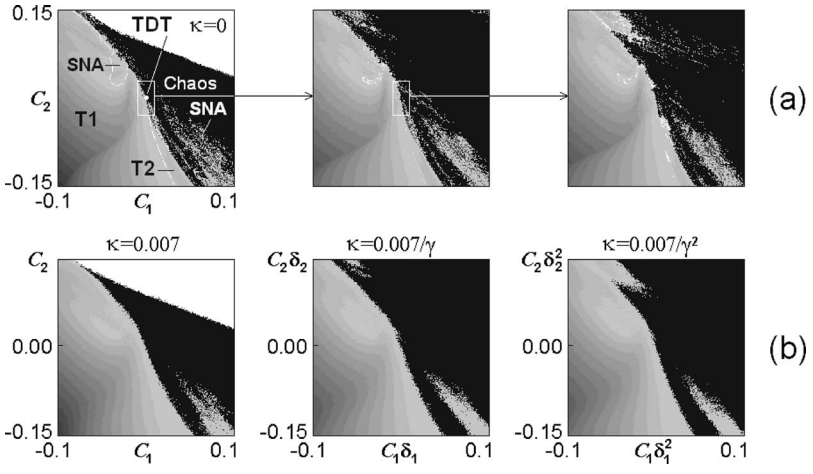

FIG. 7. Lyapunov charts demonstrating scaling in a neighborhood of the TDT critical point in scaling coordinates (27) without noise (a) and in the presence of noise (b). At each pixel of the pictures, the Lyapunov exponent was computed over approximately $1597W^{3k}$ iterations, where k is a number of the diagram in a row. Gray-scale coding is analogous to that in Fig. 1 and redefined at each new level of magnification to make the similarity clearly visible. On the first diagram (a) the nature of the main dynamical regimes is explained with inscriptions (torus $T1$, doubled torus $T2$, SNA, chaos), and the location of the TDT critical point is indicated. In the bottom row, the noise intensity parameter is decreased from one picture to another by a factor $\gamma=20.048\,664\ldots$.

$$\lambda = \lambda_c + c_1 + c_2, \quad \varepsilon = \varepsilon_c + 0.3347 c_2. \tag{27}$$

Figure 7(a) illustrates the scaling property of the Lyapunov charts for the case of absence of noise. The gray-scale coding rules are analogous to those in Fig. 1. Each next picture shows the interior of a selected rectangle from the previous diagram with enlargement by factors δ_1 and δ_2 along the horizontal and vertical axes, respectively. The Lyapunov exponent is inversely proportional to a characteristic time scale. Therefore, to outline the similarity of the pictures, the coding rule is redefined at each next level of magnification in such a way that it corresponds to a decrease of the Lyapunov exponent by a factor W^3. In the first diagram inscriptions are given, that explain the nature of dynamics in the corresponding areas (torus $T1$, doubled torus $T2$, SNA, and chaos). On subsequent diagrams the disposition of the areas is analogous. Note that all the named regimes may be found in any arbitrarily small vicinity of the TDT critical point.

Figure 7(b) shows the analogous Lyapunov charts in the presence of noise. To observe scaling, one needs additionally to decrease the noise intensity at each next step of magnification by a factor γ. For the first diagram $\kappa=0.007$; for the second and the third ones the parameter values are $\kappa = 0.007/\gamma \approx 0.000\,35$ and $\kappa \approx 0.007/\gamma^2 \approx 0.000\,017\,5$, respectively.

Good correspondence of the pictures at higher levels of magnification supports the stated scaling regularities. It is worth mentioning that in the presence of noise, the original TDT point with coordinates (2) appears to be placed inside the area of the noisy torus rather than at the border of chaotic or strange nonchaotic behavior.

V. CONCLUSION

In this paper scaling regularities associated with the effect of additive noise near the torus-doubling terminal point in a model system with golden-mean quasiperiodic driving have been discussed. A renormalization group analysis of the effect of noise was developed, and the corresponding universal constant was computed. I also presented a number of computer graphical illustrations for the scaling regularities. In particular, I put attention on the smearing of the fine structure of the critical attractor due to the presence of noise. A self-similar structure of the Lyapunov charts on the parameter plane near the TDT critical point was outlined.

I considered here only one particular representative of the universality class (forced one-dimensional quadratic map). One more example is a quasiperiodically driven supercritical circle map [7,20]. On the basis of RG argumentation it may be conjectured that the same regularities will be intrinsic to a wide class of systems, namely, the dissipative period-doubling systems under additional periodic driving with the golden-mean ratio of involved frequencies. (An example is the resistor-inductor-diode circuit studied in Ref. [9].) As expected, the results will be helpful for analysis and interpretation of experimental studies aimied at observation and investigation of behavior at the onset of complex behavior in quasiperiodically forced systems of different physical nature.

ACKNOWLEDGMENTS

The work has been performed under partial support from the Russian Foundation of Basic Research (Grant No.04-02-04011) and from the Max Planck Society.

[1] M. J. Feigenbaum, J. Stat. Phys. **19**, 25 (1978); **21**, 669 (1979); Physica D **7**, 16 (1983).
[2] P. Collet, J.-P. Eckmann, and H. Koch, Physica D **3**, 457 (1981); M. Widom, and L. P. Kadanoff, *ibid.* **5**, 287 (1982); A. P. Kuznetsov, S. P. Kuznetsov, and I. R. Sataev, *ibid.* **109**, 91 (1997).
[3] B. Hu, and J. Rudnick, Phys. Rev. Lett. **48**, 1645 (1982); J. E. Hirsch, M. Nauenberg, and D. J. Scalapino, Phys. Lett. **87A**, 391 (1982).
[4] S. J. Shenker, Physica D **5**, 405 (1982); M. J. Feigenbaum, L. P. Kadanoff, and S. J. Shenker, *ibid.* **5**, 370 (1982); D. Rand, S. Ostlund, J. Sethna, and E. D. Siggia, Phys. Rev. Lett. **49**, 132 (1982).
[5] S. P. Kuznetsov, A. S. Pikovsky, and U. Feudel, Phys. Rev. E **51**, R1629 (1995).
[6] S. Kuznetsov, U. Feudel, and A. Pikovsky, Phys. Rev. E **57**, 1585 (1998).
[7] S. Kuznetsov, E. Neumann, A. Pikovsky, and I. Sataev, Phys. Rev. E **62**, 1995 (2000).
[8] S. P. Kuznetsov, Phys. Rev. E **65**, 066209 (2002).
[9] B. P. Bezruchko, S. P. Kuznetsov, and Y. P. Seleznev, Phys. Rev. E **62**, 7828 (2000).
[10] S. P. Kuznetsov, and E. Neumann, Europhys. Lett. **61**, 20 (2003).
[11] J. Crutchfield, M. Nauenberg, and J. Rudnick, Phys. Rev. Lett. **46**, 933 (1981); B. Shraiman, C. E. Wayne, and P. C. Martin, *ibid.* **46**, 935 (1981).
[12] G. Gyorgyi and N. Tishby, Phys. Rev. Lett. **58**, 527 (1987).
[13] J. V. Kapustina, A. P. Kuznetsov, S. P. Kuznetsov, and E. Mosekilde, Phys. Rev. E **64**, 066207 (2001).
[14] A. Hamm and R. Graham, Phys. Rev. A **46**, 6323 (1992).
[15] G. Gyorgyi and N. Tishby, Phys. Rev. Lett. **62**, 353 (1989).
[16] O. B. Isaeva, and S. P. Kuznetsov, Regular Chaotic Dyn. **5**, 459 (2000).
[17] D. Fiel, J. Phys. A **20**, 3209 (1987); S.-Y. Choi and E. K. Lee, Phys. Lett. A **205**, 173 (1995).
[18] K. Kaneko, Prog. Theor. Phys. **72**, 202 (1984); A. Arneodo, Phys. Rev. Lett. **53**, 1240 (1984); S. P. Kuznetsov, JETP Lett. **39**, 133 (1984); S. P. Kuznetsov and A. S. Pikovsky, Phys. Lett. A **140**, 166 (1989).
[19] B. P. Bezruchko, S. P. Kuznetsov, A. S. Pikovsky, Ye. P. Seleznev, and U. Feudel, Appl. Nonlin. Dyn. (Saratov) **5**, 3 (1997) (in Russian); http://www.sgtnd.narod.ru/science/alphabet/eng/goldmean/tdt.htm.
[20] U. Feudel, A. S. Pikovsky, and J. Kurths, Physica D **88**, 176 (1995).